Kinetics of cardiac myosin isoforms in mouse myocardium are affected differently by presence of myosin binding protein-C

ARTICLE *in* JOURNAL OF MUSCLE RESEARCH AND CELL MOTILITY · OCTOBER 2014

Impact Factor: 2.09 · DOI: 10.1007/s10974-014-9390-0 · Source: PubMed

4 AUTHORS, INCLUDING:

Bertrand C W Tanner
Washington State University
30 PUBLICATIONS **101** CITATIONS
SEE PROFILE

Yuan Wang
University of Vermont
18 PUBLICATIONS **312** CITATIONS
SEE PROFILE

J Muscle Res Cell Motil
DOI 10.1007/s10974-014-9390-0

ORIGINAL PAPER

Kinetics of cardiac myosin isoforms in mouse myocardium are affected differently by presence of myosin binding protein-C

Bertrand C. W. Tanner · Yuan Wang · Jeffrey Robbins · Bradley M. Palmer

Received: 3 July 2014 / Accepted: 22 September 2014

Abstract We tested whether cardiac myosin binding protein-C (cMyBP-C) affects myosin cross-bridge kinetics in the two cardiac myosin heavy chain (MyHC) isoforms. Mice lacking cMyBP-C (t/t) and transgenic controls ($WT^{t/t}$) were fed L-thyroxine (T4) to induce 90/10 % expression of α/β-MyHC. Non-transgenic (NTG) and t/t mice were fed 6-*n*-propyl-2-thiouracil (PTU) to induce 100 % expression of β-MyHC. Ca^{2+}-activated, chemically-skinned myocardium underwent length perturbation analysis with varying [MgATP] to estimate the MgADP release rate (k_{-ADP}) and MgATP binding rate (k_{+ATP}). Values for k_{-ADP} were not significantly different between t/t_{T4} ($102.2 \pm 7.0\ s^{-1}$) and $WT^{t/t}_{T4}$ ($91.3 \pm 8.9\ s^{-1}$), but k_{+ATP} was lower in t/t_{T4} ($165.9 \pm 12.5\ mM^{-1}\ s^{-1}$) compared to $WT^{t/t}_{T4}$ ($298.6 \pm 15.7\ mM^{-1}\ s^{-1}$, $P < 0.01$). In myocardium expressing β-MyHC, values for k_{-ADP} were higher in t/t_{PTU} ($24.8 \pm 1.0\ s^{-1}$) compared to NTG_{PTU} ($15.6 \pm 1.3\ s^{-1}$, $P < 0.01$), and k_{+ATP} was not different. At saturating [MgATP], myosin detachment rate approximates k_{-ADP}, and detachment rate decreased as sarcomere length (SL) was increased in both t/t_{T4} and $WT^{t/t}_{T4}$ with similar sensitivities to SL. In myocardium expressing β-MyHC, detachment rate decreased more as SL increased in t/t_{PTU} ($21.5 \pm 1.3\ s^{-1}$ at 2.2 μm and $13.3 \pm 0.9\ s^{-1}$ at 3.3 μm) compared to NTG_{PTU} ($15.8 \pm 0.3\ s^{-1}$ at 2.2 μm and $10.9 \pm 0.3\ s^{-1}$ at 3.3 μm) as detected by repeated-measures ANOVA ($P < 0.01$). These findings suggest that cMyBP-C reduces MgADP release rate for β-MyHC, but not for α-MyHC, even as the number of cMyBP-C that overlap with the thin filament is reduced to zero. Therefore, cMyBP-C appears to affect β-MyHC kinetics independent of its interaction with the thin filament.

Keywords Cross-bridge · Time-on · Transgenic

Introduction

Cardiac myosin binding protein-C (cMyBP-C) augments thick filament structural integrity (Zoghbi et al. 2008) and stiffness (Nyland et al. 2009) and can bind actin, myosin and titin (Bhuiyan et al. 2012; Freiburg and Gautel 1996). These structural characteristics of cMyBP-C play a role in stiffening the contracting myocardium, facilitating cardiac relaxation, prolonging myosin cross-bridge lifetime t_{on} and slowing unloaded shortening velocity, as demonstrated at the whole heart (Carrier et al. 2004; Harris et al. 2002; McConnell et al. 1999), myocardial (Korte et al. 2003; Palmer et al. 2011; Stelzer et al. 2006) and molecular levels (Previs et al. 2012). It is not yet known if cMyBP-C influences specific nucleotide-dependent transition rates in the myosin cross-bridge cycle. Given previous findings that myosin ATPase, loaded and unloaded shortening velocity, myosin cross-bridge detachment rate and MgADP release rate differ by roughly four-fold between cardiac α- and β-MyHC isoforms in the context of an intact myofilament

B. C. W. Tanner · Y. Wang · B. M. Palmer (✉)
Department of Molecular Physiology and Biophysics, University of Vermont, 122 HSRF, 149 Beaumont Ave., Burlington, VT 05405, USA
e-mail: bmpalmer@uvm.edu

Present Address:
B. C. W. Tanner
Department of Integrative Physiology and Neuroscience, Washington State University, Pullman, WA 99164, USA

J. Robbins
Department of Pediatrics, Cincinnati Children's Hospital Medical Center, Cincinnati, OH 45229, USA

Published online: 07 October 2014

lattice (Korte et al. 2005; Rundell et al. 2005; Wang et al. 2013), rather than the two-fold difference observed using isolated cardiac myosin (Palmiter et al. 1999; Pereira et al. 2001), we hypothesized that the structural protein cMyBP-C would influence cross-bridge kinetics in a myosin isoform-dependent manner.

The present study examines myosin cross-bridge rates of MgADP release and MgATP binding in left ventricular (LV) myocardial strips isolated from mice lacking cMyBP-C versus controls, which have been matched for MyHC isoform using thyroid hormone manipulation. We also examined the sensitivity of myosin cross-bridge detachment rate to sarcomere length (SL) in the two MyHC isoforms. Our results suggest that the presence of cMyBP-C in the myofilament lattice reduces the MgADP release rate in the β-MyHC isoform but not in the α-MyHC and that cMyBP-C has this effect on the β-MyHC isoform as the sarcomere lengthens beyond where cMyBP-C can interact with the thin filament (Pfuhl and Gautel 2012). The possible structural bases of these effects are discussed.

Materials and methods

Animal models

All procedures were reviewed and approved by the Institutional Animal Care and Use Committees of The University of Vermont College of Medicine and The University of Cincinnati Children's Hospital and complied with the *Guide for the Use and Care of Laboratory Animals* published by the National Institutes of Health. All mice were of the FVB background. Male, transgenic mice lacking cMyBP-C (t/t) or expressing full length wild-type cMyBP-C in a t/t background ($WT^{t/t}$) were acquired from University of Cincinnati (Sadayappan et al. 2005). Male, non-transgenic (NTG) mice were acquired from Charles River (Wilmington, MA). $WT^{t/t}$ (n = 4) and t/t (n = 5) mice were fed 3 mg/kg L-thyroxine (T4) for 10 days, which emulated hyperthyroidism to upregulate α-MyHC expression in the LV for both genotypes (Palmer et al., 2011). NTG (n = 5) and t/t (n = 5) mice were fed an iodine-deficient 0.15 % propylthiouracil (PTU) diet (Harlan Teklad, Indianapolis, IN) for at least 12 weeks, which resulted in hypothyroidism and an upregulation of β-MyHC expressed in the LV (Palmer et al. 2004; Wang et al. 2013). Mice were anaesthetized by inhalation of isoflurane (1.5–3 % mg/kg), following which hearts were immediately excised and placed in preoxygenated (95 % O_2–5 % CO_2) Krebs solution at room temperature. LVs were placed in 10 % paraformaline and morphology was assessed by H & E and Mason's trichrome stain (American Histolabs, Gaithersburg, MD).

Myosin isoform content

Myosin isoform content in the LV was determined by gel electrophoresis (Reiser and Kline 1998) using Fluormax-2 Imaging analysis (Bio-Rad, Hercules CA). Total optical densities of bands were corrected for background using ImageJ v1. 38 (NIH, USA).

Solutions

Chemicals and reagents were obtained from Sigma Corp. (St. Louis, MO) unless otherwise noted. Krebs solution contained (mmol/L) 137 Na^+, 153 Cl^-, 5.4 K^+, 0.2 Ca^{2+}, 1.3 Mg^{2+}, 10 Glucose, 10 Hepes, 30 BDM, pH 7.4. Solutions for skinned strips were formulated by solving equations describing ionic equilibria (Godt and Lindley 1982). Relaxing solution: pCa 8.0 [$pCa = \log_{10}(Ca^{2+})$], 5 EGTA, 5 MgATP, 1 Mg^{2+}, 35 phosphocreatine (PCr), 300 U/mL creatine kinase (CK), ionic strength 200, pH 7.0. Activating solution: same as relaxing with pCa 4.0. Rigor solution: same as relaxing with pCa 4.8 and 0 MgATP. Skinning solution: same as relaxing without CK, with 1 % Triton-X100 wt/vol and 50 % glycerol wt/vol. Storage solution: same as skinning without Triton, with 10 μg/mL leupeptin. Alkaline phosphatase (AP) solution: same as relaxing solution with 6 U/mL recombinant AP from E-coli (P-4252).

Skinned myocardial strips

Skinned papillary muscle strips were prepared and studied as previously described (Wang et al. 2013). Immediately before mechanical analysis, all strips were incubated for 10 min in AP solution at room temperature. The combination of extended BDM incubation and AP pretreatment of experimental and control groups provides a useful approach to better match the phosphorylation status of sarcomeric proteins by reducing any differential phosphorylation profiles at troponin-I serines-21/22 and myosin regulatory light chain serine-19, as demonstrated by phospho-specific antibodies (Wang et al. 2013). Strips were mounted between a piezoelectric motor (P841.60, Physik Instrumente, Auburn, MA) and a strain gauge (AE801, Kronex, Walnut Creek, CA), lowered into a 30 μL droplet of relaxing solution maintained at 17 °C, and stretched to 2.2 μm SL as measured by digital Fourier Transform (IonOptix Corp, Milton, MA). Strips were calcium activated to pCa 4.8, following which either rigor solution was exchanged for activating solution to lower [MgATP] from 5 to <0.01 mM or SL was increased from 2.2 to 3.3 μm. In the latter case, SL was visualized up to 2.8 μm and then stretched by 15 % to reach 3.3 μm, which could not be reliably visualized. At least two strips per heart underwent

either the rigor titration or SL extension protocol, and data were averaged for each heart.

Mechanical system analysis

Sinusoidal length perturbations of amplitude 0.125 % strip length were applied at 0.125–100 Hz (Wang et al. 2013). Elastic and viscous moduli as a function of angular frequency ω, $E(\omega)$ and $V(\omega)$, were used to define the complex modulus, $Y(\omega) = E(\omega) + iV(\omega)$ where $i = \sqrt{-1}$. Fitting Eq. 1 to the entire frequency range of moduli values provided estimates of six model parameters (A, k, B, $2\pi b$, C, $2\pi c$).

$$Y(\omega) = A(i\omega)^k - B\left(\frac{i\omega}{2\pi b + i\omega}\right) + C\left(\frac{i\omega}{2\pi c + i\omega}\right), \qquad (1)$$

The A-term in Eq. 1 reflects the visco-elastic mechanical response of passive elements in the muscle. In our interpretation, parameter A represents the combined mechanical stiffness of the parallel elastic elements, the myofilaments and the number of strongly bound cross-bridges, and k describes the degree of the viscoelasticity in the response, where $k \rightarrow 0$ is a purely elastic response and $k \rightarrow 1$ is a purely viscous response. The B- and C-terms of Eq. 1 reflect enzymatically driven myosin cross-bridge formation in activated muscle. Parameters B and C reflect the number of cross-bridges formed × their mean stiffness (or total myosin cross-bridges available × duty ratio × mean stiffness), and the rate parameters $2\pi b$ and $2\pi c$ reflect cross-bridge kinetics sensitive to biochemical perturbations known to affect enzymatic activity, such as [MgATP], [MgADP], or [Pi]. The B-term underlies processes of cross-bridge attachment or force generation, such that $2\pi b$ describes rate of force generation and has been proposed to be due to cross-bridge recruitment (Campbell et al. 2004) or the characteristic rates of myosin isomerization including Pi-dependent cross-bridge detachment (Kawai and Halvorson 1991; Zhao and Kawai 1993). The C-term underlies processes of cross-bridge detachment or force decay, such that $2\pi c$ describes to the rate of cross-bridge detachment, which is inversely related to the average myosin attachment time, $t_{on} = (2\pi c)^{-1}$ (Wang et al. 2013).

Myosin enzyme kinetics

Assuming that the myosin t_{on} consists almost entirely of the time periods of myosin ADP and rigor states, the myosin detachment rate, $2\pi c$, is therefore related to MgATP-dependent parameters of myosin detachment as explained in detail in Tyska and Warshaw and implemented in our previous publication (Tyska and Warshaw 2002; Wang et al. 2013):

$$2\pi c = \frac{k_{-ADP}[MgATP]}{\frac{k_{-ADP}}{k_{+ATP}} + [MgATP]}, \qquad (2)$$

where k_{-ADP} = rate of MgADP release and the asymptotic, maximal myosin detachment rate (s^{-1}), k_{+ATP} = rate of MgATP binding per MgATP concentration (M^{-1} s^{-1}), and the ratio (k_{-ADP}/k_{+ATP}) = concentration of MgATP producing half the maximal myosin detachment rate [$(MgATP)_{50}$]. One or two strips per heart underwent these measured of MgADP and MgATP kinetics.

Statistical analysis

Multiple measurements from the same heart were averaged to provide a single measure for that heart. All values are mean ± SE, where n represents the number of hearts. Moduli data were fit to Eq. 1 using IDL (v. 7, Exelis Visual Information Solutions, Inc.; Boulder, CO) as previously described (Wang et al. 2013). The differential sensitivity of myosin detachment rate to varying SL was analyzed using repeated-measures ANOVA with SL as within-subject variable and genotype as between-subject variable. Statistical analyses were performed using SPSS (v.20.0, IBM SPSS Statistics, Chicago, IL).

Results

Cardiac morphology and myosin isoform profiles

Qualitative visual assessment of LV morphology suggests the effects of a 10 day T4 diet did not change LV structure in the $WT^{t/t}_{T4}$ compared to a normal mouse LV evidenced by the relatively well organized nuclei (stained blue by H & E, Fig. 1a) and myocytes (stained red by H & E, Fig. 1a) with no fibrosis (stained blue by trichrome, Fig. 1b). There was also significant myocyte disarray and fibrosis in the t/t_{T4} compared to $WT^{t/t}_{T4}$ mice (Fig. 1a–d). These findings are consistent with those reported for cMyBP-C knockout mice (Carrier et al. 2004; Harris et al. 2002; McConnell et al. 1999) and $WT^{t/t}$ (Sadayappan et al. 2005).

The NTG_{PTU} hearts showed limited myocyte disarray (Fig. 1e), whereas the t/t_{PTU} hearts display a moderate level of myocyte disarray due to the loss of cMyBP-C (Fig. 1g). Both NTG_{PTU} and t/t_{PTU} also demonstrate cardiac fibrosis, as indicated by blue stain in Fig. 1f and h, observed after 12 weeks of PTU diet and subsequent hypothyroidism. These findings suggest that secondary responses to the lack of cMyBP-C led to some differences in myocyte disarray.

Consistent with our previous observations (Palmer et al. 2011), regimens of T4 diet successfully resulted in complimentary LV α-MyHC content in the $WT^{t/t}_{T4}$ (87 ± 1 %)

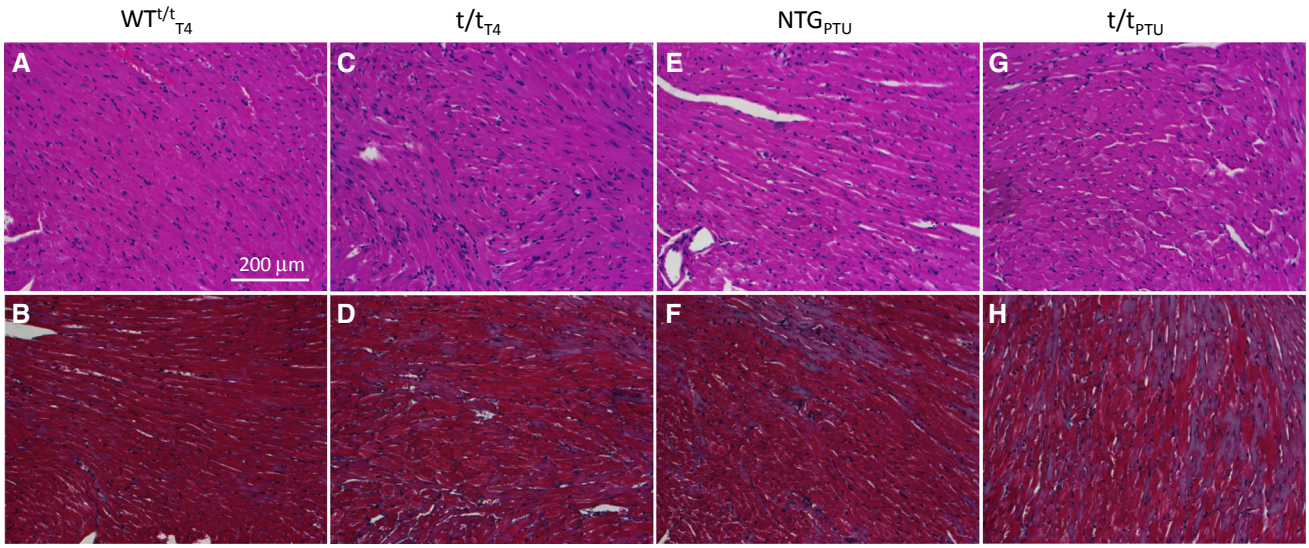

Fig. 1 Cardiac morphology assessed by H & E and Mason's trichrome staining. The $WT^{t/t}_{T4}$ shows normal myocyte disarray and fibrosis (**a**, **b**), comparable to that observed for a normal mouse, while the t/t_{T4} myocardium displayed disarray and fibrosis (**c**, **d**) relative to the $WT^{t/t}_{T4}$. These observations in the T4-fed mice were similar to those expected without any special diet. After 12 weeks of hypothyroidism due to PTU diet, however, both NTG_{PTU} (**e**, **f**) and t/t_{PTU} (**g**, **h**) show significant fibrosis as indicated by *blue color* in the trichrome stain (**f**, **h**)

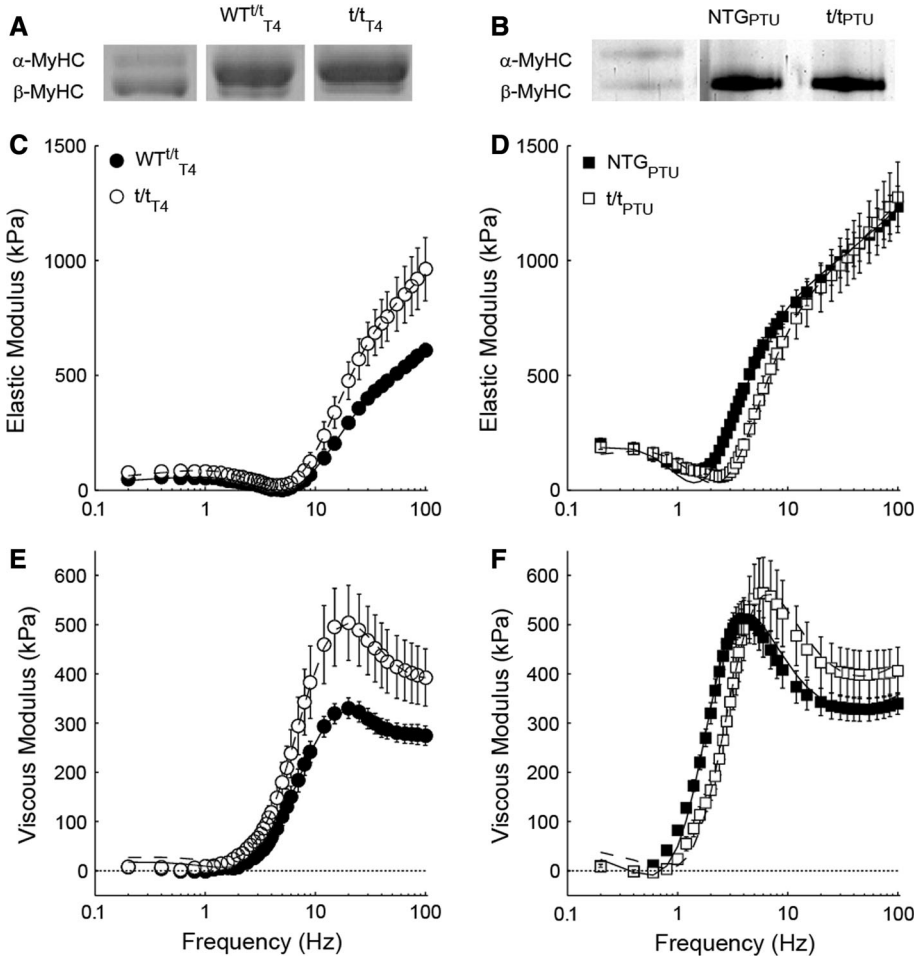

Fig. 2 Complex modulus of skinned myocardial strips from mice expressing α- versus β-MyHC. Gel electrophoresis of left ventricle tissue homogenate stained with *Coomassie-Blue* demonstrate (**a**) a ~90/10 % α/β-MyHC expression ratio for T4-fed transgenic control mice $\left(WT^{t/t}_{T4}\right)$ and mice lacking cMyBP-C (t/t_{T4}), and **b** ~100 % β-MyHC expression in PTU-fed non-transgenic mice (NTG_{PTU}) and t/t lacking cMyBP-C (t/t_{PTU}). Bands for T4-fed mice are from the same gel, but not contiguous lanes, whereas bands for PTU-fed mice are from contiguous lanes of the same gel. Frequency characteristics of the elastic (**c**, **d**) and viscous (**e**, **f**) moduli of myocardium at maximum calcium activation and 5 mM MgATP are similar between groups bearing α-MyHC, but noticeably different between groups bearing β-MyHC

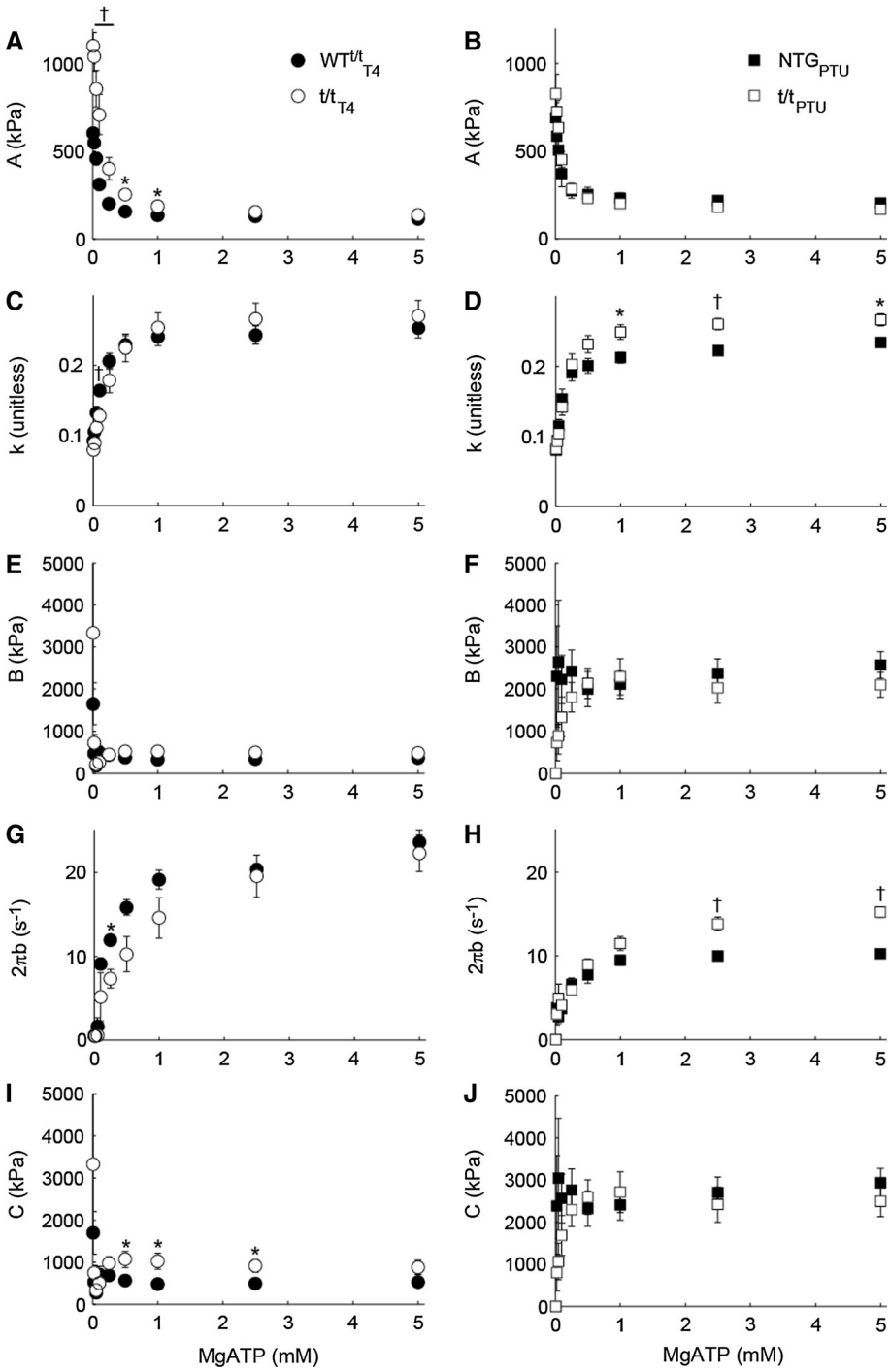

Fig. 3 Effect of [MgATP] on parameters of Eq. 1. For T4 and PTU-fed populations, myocardial viscoelastic stiffness rose as [MgATP] was lowered as reflected by the reduction in magnitude A (**a**, **b**) and became increasingly elastic as reflected by the decrease in k (**c**, **d**). The rate of force redevelopment $2\pi b$ was reduced as [MgATP] was lowered among all populations (**g**, **h**), while $2\pi b$ was ~2-fold faster for α- versus β-MyHC. Compared to other model parameters, the magnitudes B (**e**, **f**) and C (**i**, **j**) were relatively insensitive to [MgATP]. $^{\dagger}P < 0.01$; $^{*}P < 0.05$ between experimental and control groups within a panel

and t/t_{T4} (89 ± 1 %) populations (Fig. 2a). The PTU diet resulted in 100 % expression of β-MyHC in both the NTG_{PTU} and t/t_{PTU} populations (Fig. 2b).

It should be noted that we used the $WT^{t/t}$ as a control for t/t in the α-MyHC background, because feeding T4 to NTG mice results in 0 % β-MyHC and therefore does not match the ~10 % β-MyHC isoform content in the t/t_{T4}. Furthermore, we did not use the $WT^{t/t}_{T4}$ as a control for t/t in the β-MyHC background, because PTU fed to the $WT^{t/t}$ would result in the loss of cMyBP-C from the sarcomere because cMyBP-C is expressed with the α-MyHC promoter in this transgenic mouse (Sadayappan et al. 2005). Further consideration of the control mice are presented in the Limitations subsection of the "Discussion" section.

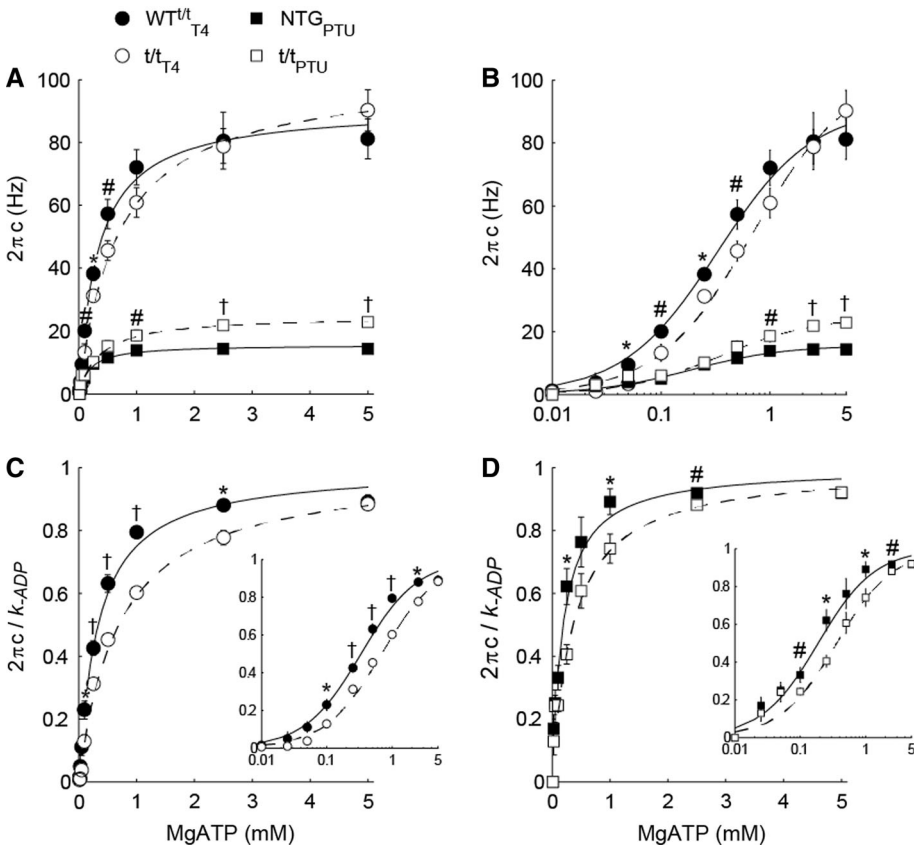

Fig. 4 MgATP-sensitivity of myosin cross-bridge detachment rate $2\pi c$ at maximal Ca^{2+} activation (pCa 4.8). **a** $2\pi c$ was elevated as [MgATP] increased from <0.01 to 5 mM in skinned myocardial strips from thyroxin-fed and PTU-fed mice. *Solid* (controls) and *dashed* (t/t) lines show fits to Eq. 2. Normalizing $2\pi c$ to the asymptotic MgADP release rate (k_{-ADP}; Table 2) demonstrates relative sensitivities to [MgATP] for each population, effectively highlighting (**b**) the ~ 2-fold faster MgATP release rate (k_{+ATP}) from α-MyHC for $WT^{t/t}_{T4}$ vs. t/t_{T4} and **c** the ~ 1.5-fold faster k_{-ADP} from β-MyHC for NTG_{PTU} versus t/t_{PTU}. *Insets* within panels **c** and **d** show data versus log[MgATP]. $^{\dagger}P < 0.01$; $^{*}P < 0.05$ between experimental and control groups within a panel

Myosin enzyme kinetics

In the $WT^{t/t}_{T4}$ and t/t_{T4} myocardium expressing predominately α-MyHC, the elastic and viscous moduli at saturating [MgATP] exhibited similar frequency characteristics between the genotypes (Fig. 2c, e). In contrast, the respective dips and shoulders of the elastic and viscous moduli-frequency responses were shifted to higher frequencies in the t/t_{PTU} compared to NTG_{PTU} controls expressing β-MyHC (Fig. 2d, f), indicating faster cross-bridge kinetics for t/t_{PTU} vs. NTG_{PTU}. Complex moduli were fit to Eq. 1 to estimate model parameters describing viscoelastic muscle mechanics and rate constants associated with cross-bridge kinetics as [MgATP] decreased from 5 to ≥0.1 mM. Although not shown here, the moduli-frequency relationship shifted towards lower frequencies as [MgATP] was reduced, similar to that illustrated in the previous report (Wang et al. 2013), which reflects a prolonged myosin cross-bridge rigor state at lower [MgATP].

For all populations, the magnitude *A* was enhanced and the index *k* was depressed as [MgATP] was reduced. These findings correspond to a greater number and longer duration strongly bound cross-bridges (Fig. 3a, b) and a more elastic versus viscous characteristic (Fig. 3c–e) of the muscle, respectively, as [MgATP] decreased. Magnitudes *B* and *C* displayed high variation particularly as [MgATP] fell below 0.5 mM (Fig. 3e, f and i, j). The rate of force development $2\pi b$ rose to a maximum value at saturating [MgATP] and was faster in the α-MyHC compared to β-MyHC as would be expected for these isoforms (Fig. 3g, h). For all populations, cross-bridge detachment rate $2\pi c$ rose hyperbolically with increasing [MgATP] (Fig. 4a). These $2\pi c$-[MgATP] relationships were fit to Eq. 2 to estimate MgADP release (k_{-ADP}) and MgATP attachment (k_{+ATP}) rates for α- and β-MyHC in the presence and absence of cMyBP-C (Table 1).

Values for k_{-ADP} did not differ between $WT^{t/t}_{T4}$ and t/t_{T4}, while k_{+ATP} was nearly twice as fast in the $WT^{t/t}_{T4}$ compared to t/t_{T4} (Table 1). This effect of cMyBP-C on the rate MgATP binding can be observed via higher $2\pi c$ values in the $WT^{t/t}_{T4}$ at sub-saturating [MgATP] (Fig. 4a, c). In contrast, values for k_{-ADP} were significantly higher in t/t_{PTU} compared to NTG_{PTU}, and k_{+ATP} did not differ between these genotypes expressing β-MyHC. These findings show that cMyBP-C does not significantly affect MgADP release rate for α-MyHC in the intact myofilament lattice, and that cMyBP-C would not be expected to affect α-MyHC cross-bridge t_{on} under physiological conditions that include saturating [MgATP] and an intact myofilament lattice. In contrast, these findings suggest that cMyBP-C slows MgADP

Table 1 Parameters representing myosin enzyme kinetics were estimated by fitting myosin cross-bridge detachment rate ($2\pi c$) versus MgATP relationships to Eq. 2

	$WT^{t/t}_{T4}$	t/t_{T4}	NTG_{PTU}	t/t_{PTU}
k_{-ADP} (s^{-1})	91.3 ± 8.9	102.2 ± 7.0	15.6 ± 1.3	24.8 ± 1.0†
k_{+ATP} (mM^{-1} s^{-1})	298.6 ± 15.7	165.9 ± 12.5†	99.8 ± 20.0	77.5 ± 14.5
t_{-ADP} (ms)	11.3 ± 1.0	10.0 ± 0.6	65.6 ± 10.6	40.6 ± 17.1†
$MgATP_{50}$ (μM)	333 ± 34	689 ± 25†	188 ± 45	361 ± 58*

* $P < 0.05$; † $P < 0.01$ against respective controls

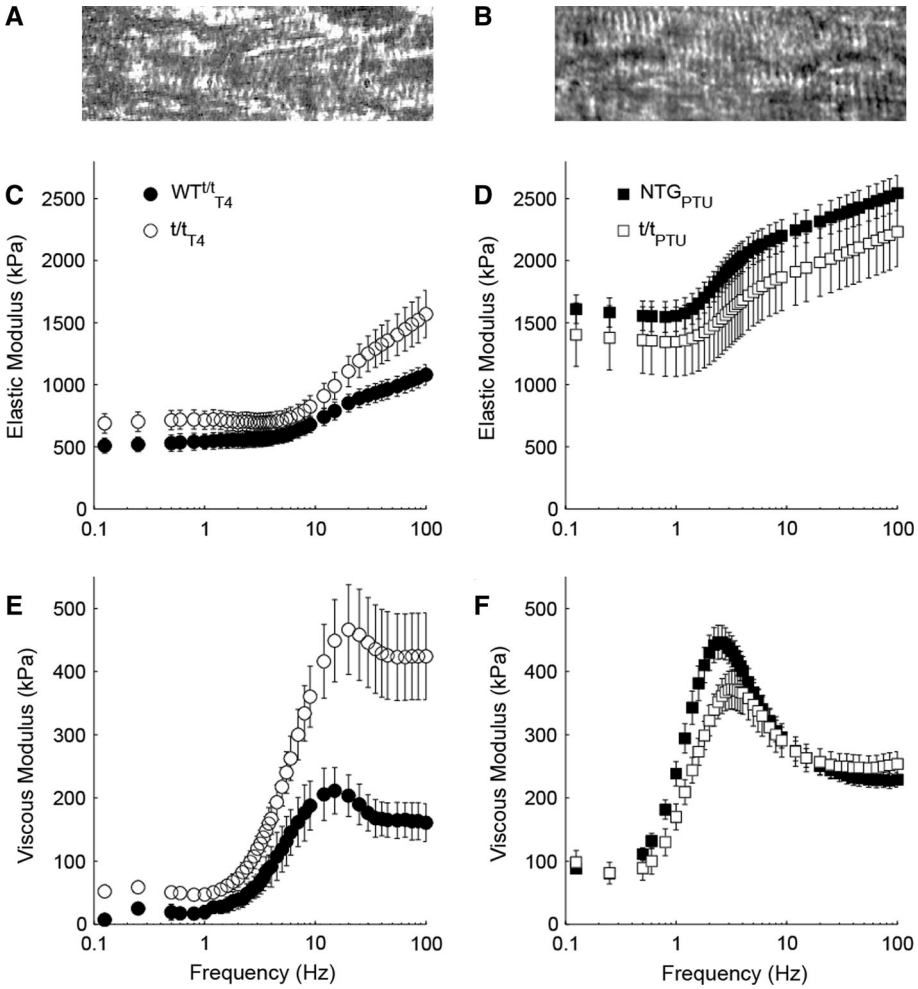

Fig. 5 Complex modulus at 3.3 μm sarcomere length. Bright field images of papillary muscle illustrate visible sarcomeres at 2.2 μm (**a**) and 2.8 μm (**b**) sarcomere length. Further lengthening to 3.3 μm did not routinely permit visualization of sarcomeres. Frequency characteristics of the elastic (**c**, **d**) and viscous (**e**, **f**) moduli of mouse myocardium were similar between groups bearing α-MyHC, but noticeably different between groups bearing β-MyHC. Specifically, myocardium lacking cMyBP-C in the t/t_{PTU} display higher frequency characteristics compared to NTG_{PTU}

release in the β-MyHC to prolong the myosin cross-bridge t_{on} under physiological conditions.

Myosin cross-bridge detachment rate and sarcomere length

No differences in isometric tension were observed between t/t mice and their respective controls. Passive tension values (mean ± SE in kPa, pCa 8.0, 5 mM MgATP) were 5.5 ± 0.1 and 5.6 ± 0.4 for $WT^{t/t}_{T4}$ and t/t_{T4}, respectively, at 2.2 μm SL and then 27.2 ± 6.7 and 22.9 ± 3.0 for $WT^{t/t}_{T4}$ and t/t_{T4}, respectively, at 3.3 μm SL. Passive tension in the myocardial strips bearing β-MyHC were 5.3 ± 0.3, and 5.5 ± 0.1 for NTG_{PTU} and t/t_{PTU}, respectively, at 2.2 μm and then 95.9 ± 9.1 and 72.7 ± 17.3 for NTG_{PTU}, and t/t_{PTU}, respectively, at 3.3 um SL.

Developed tension values (pCa 4.8 tension – passive tension) were 24.9 ± 2.2 kPa and 29.6 ± 2.0 kPa for $WT^{t/t}_{T4}$ and t/t_{T4}, respectively, at 2.2 μm SL and then 19.2 ± 2.4 kPa and 19.1 ± 1.7 kPa for $WT^{t/t}_{T4}$ and t/t_{T4},

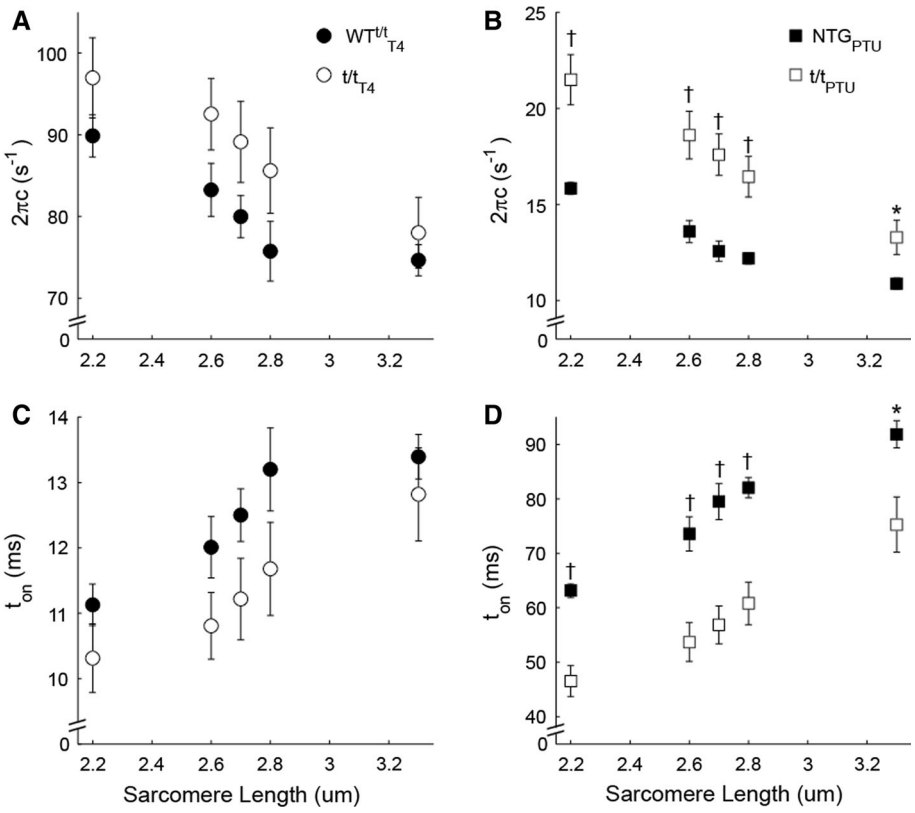

Fig. 6 Effect of sarcomere length on myosin cross-bridge detachment rate $2\pi c$. **a** Cross-bridge detachment rate decreased and **c** cross-bridge attachment duration (t_{on}) increased for α-MyHC with increasing sarcomere length, independent of the presence $\left(WT^{t/t}_{T4}\right)$ or absence (t/t_{T4}) of cMyBP-C. **b** Detachment rate was faster and **d** t_{on} was shorter for β-MyHC in the absence of cMyBP-C at all sarcomere lengths examined, including 3.3 μm where there is no overlap between the *thin filament* and the *thick filament* C-zone. The sensitivity of detachment rate reduction with increasing sarcomere length was greater in the absence (t/t_{PTU}) rather than presence (NTG_{PTU}) of cMyBP-C. $^{\dagger}P < 0.01$; $^{*}P < 0.05$ between experimental and control groups

Table 2 Results of repeated-measures ANOVA applied to detachment rate $2\pi c$ detected at increasing sarcomere lengths (SL)

	$WT^{t/t}_{T4}$	NTG_{PTU} versus t/t_{PTU}
SL	$<0.001^{\dagger}$	$<0.001^{\dagger}$
Genotype	0.148	$0.004^{\dagger}$
SL × genotype	0.307	$0.002^{\dagger}$

† $P < 0.01$

respectively, at 3.3 μm SL. Developed tension in the myocardial strips bearing β-MyHC were 21.6 ± 1.3 kPa, and 16.6 ± 2.5 kPa for NTG_{PTU} and t/t_{PTU}, respectively, at 2.2 μm and then 49.9 ± 2.9 kPa and 50.9 ± 10.1 kPa for NTG_{PTU} and t/t_{PTU}, respectively, at 3.3 um SL. These data for isometric tension are indicative of comparable activation of a muscle strip across the range of 2.2–3.3 μm SL.

It is visually apparent that the elastic and viscous moduli were raised in magnitude and, more importantly, shifted to lower frequencies as SL was increased from 2.2 μm (Fig. 2)–3.3 μm (Fig. 5). In myocardium expressing predominately α-MyHC, myosin detachment rate $2\pi c$ was not statistically different between t/t_{T4} and $WT^{t/t}_{T4}$ (Fig. 6a; $P < 0.148$ for genotype main effect, Table 2), but increasing SL from 2.2–3.3 μm reduced $2\pi c$ by ~15 % for both genotypes ($P < 0.001$ for SL main effect). Detachment rate was not differentially affected by the absence of cMyBP-C in t/t_{T4} versus $WT^{t/t}_{T4}$ ($P = 0.307$ for SL × genotype interaction), suggesting that cMyBP-C did not influence α-MyHC detachment rate as SL varied.

In myocardium expressing β-MyHC, cross-bridge detachment rate was significantly higher in the t/t_{PTU} compared to NTG_{PTU} over the entire range of SL examined (Fig. 6b; $P = 0.004$ for genotype main effect, Table 2), including 3.3 μm where there is no overlap between the thin filament and the C-zone of thick filaments, where cMyBP-C resides. Increases in SL more greatly reduced $2\pi c$ for t/t_{PTU} than for NTG_{PTU} ($P = 0.002$ for SL × genotype interaction). These results suggest that the presence of cMyBP-C reduces myosin detachment rate in β-MyHC both with and without overlap between the thin filament and the C-zone. Furthermore, the relative reduction in β-MyHC detachment rate with increasing SL was amplified in the absence of cMyBP-C.

Discussion

This study presents the effects of cMyBP-C on MgATP-dependent kinetics of the two cardiac myosin isoforms in mouse myocardium. In the α-MyHC k_{-ADP} was not measurably affected by the absence of cMyBP-C, but in β-MyHC k_{-ADP} was enhanced ~35 % with the absence of

cMyBP-C. Lengthening the sarcomere from 2.2 to 3.3 μm reduced the cross-bridge detachment rate in α-MyHC by ~15 %, but this effect was not sensitive to the absence of cMyBP-C. Cross-bridge detachment rate in the β-MyHC, in contrast, was reduced ~30 % with sarcomere lengthening in the presence of cMyBP-C and ~40 % in the absence of cMyBP-C. These findings collectively suggest that under physiological [MgATP] conditions cMyBP-C reduces β-MyHC detachment rate through some structural role that is independent of any possible interaction with the thin filament.

MyHC kinetics measured under isometric conditions

We would contend that the cardiac sarcomere in our assay is effectively isometric and the possible viscous effects of cMyBP-C binding to the thin filament are minimal. The length perturbation analysis technique used in this study relies upon oscillating the ~1,100 nm half-sarcomere an amplitude of ~1.3 nm. The N-terminus of cMyBP-C emanating from the surface of the thick filament is on the order of 29–34 nm long and can easily span the distance to the thin filament approximately 8–12 nm away (Luther et al. 2011; Oshima et al. 2012). Even with a maximum oscillatory excursion of 2.6 nm of the thin filament relative to the thick filament, cMyBP-C attached to the thin filament would not be expected to experience a significant strain and might be slack throughout. Thus, the concept that cMyBP-C contributes a viscous load to slow loaded sarcomere shortening (Korte et al. 2003), the rate of force development (Stelzer et al. 2006), or unloaded shortening velocity and actin velocity (Hofmann et al. 1991; Previs et al. 2012; Razumova et al. 2006; Saber et al. 2008) has limited relevance in interpreting the kinetic measurements of the current study. Furthermore, our observation that α-MyHC detachment rate at 100 μM [MgATP] is faster in the presence of cMyBP-C (Fig. 4) does not agree with isolated myosin or thick filament assays demonstrating that cMyBP-C slows unregulated actin sliding velocity (Previs et al. 2012; Razumova et al. 2006; Weith et al. 2012). Based on the above observations, we therefore speculate that cMyBP-C influences strain-dependent cross-bridge kinetics within the intact myofilament lattice through its effects on myofilament lattice stiffness and not necessarily though its interaction with the thin filament. Still, cMyBP-C may also contribute a viscous load to actin filaments when significant translation occurs via dynamic changes in SL during shortening and relaxation.

cMyBP-C as structural modulator of MyHC kinetics

Mechanical characteristics of the sarcomere influence myosin cross-bridge kinetics and thereby play a role in dictating contraction dynamics of striated muscle (Hunter et al. 1998; Land et al. 2012; Tanner et al. 2007). We had previously observed that a loss of cMyBP-C leads to a collapsed myofilament lattice in the t/t compared to controls (Palmer et al. 2011), which would be expected to reduce k_{-ADP} and prolong t_{on} (Tanner et al. 2012). Therefore, any collapse in lattice spacing with the loss of cMyBP-C in the current study is unlikely to underlie the enhanced k_{-ADP} observed in the β-MyHC in the t/t_{PTU}. We would instead suggest that, because cMyBP-C accounts for ~40 % of the flexural rigidity of thick filament in part through its binding to titin (Nyland et al. 2009) and contributes to the radial rigidity of the myofilament lattice (Palmer et al. 2011), the enhanced structural stiffness of the myofilaments afforded by cMyBP-C would be expected to influence the distribution of strain throughout the sarcomere and alter the load borne by bound cross-bridges throughout their attached lifetime. The reduction in stiffness properties of these structures with a loss of cMyBP-C will result in greater deformation of the cMyBP-C-dependent structures and a commensurately reduced deformation of the myosin head, including the nucleotide binding pocket, thereby affecting the rates k_{-ADP} and k_{+ATP}.

We speculate at this time that the observed changes in k_{-ADP} and k_{+ATP} due to loss of cMyBP-C reflect stiffness-dependencies of k_{-ADP} and k_{+ATP} in the respective myosin isoforms. Specifically, the absence of cMyBP-C may lead to greater deformation of the myofilaments and less deformation of the myosin head, thus underlying the increased k_{-ADP} in β-MyHC and reduced k_{+ATP} in the α-MyHC. We would not expect cMyBP-C to interact with the subfragment-2 or light-meromyosin portions of MyHC differently between the two cardiac MyHC isoforms, as these myosins reportedly bear identical amino acid sequences in these binding regions (Bhuiyan et al. 2012; Gruen and Gautel 1999).

Using skinned myocardial preparations, measures of myosin ATPase, loaded and unloaded shortening velocities, cross-bridge t_{on} and cross-bridge detachment rate differ by roughly four-fold between cardiac α- and β-MyHC isoforms (Korte et al. 2005; Rundell et al. 2005; Wang et al. 2013), rather than the two-fold difference observed using isolated cardiac myosin (Palmiter et al. 1999; Pereira et al. 2001). These observations suggest that the intact myofilament lattice and sarcomeric structural proteins play important roles in dictating cross-bridge rates of nucleotide release and binding that vary with MyHC isoform, despite identical structures of the nucleotide binding pockets. The functional interchangeability of the structurally dissimilar loop-1 and loop-2 in the mouse cardiac isoforms (Krenz et al. 2003) underscores the likelihood that myofilament structure plays a significant role in governing myosin kinetics.

With this in mind, the current study suggests that β-MyHC is much more sensitive to structural perturbation in the myofilament lattice than α-MyHC, at least in mouse myocardium. This could follow from β-MyHC being attached ~ four-times longer than α-MyHC, such that any reduced load borne due to diminished thick filament stiffness in the absence of cMyBP-C is manifest effectively as a more 'assistive' load resulting in less deformation of the nucleotide binding pocket in β-MyHC of the t/t_{PTU} myocardium (Kad et al. 2007; Veigel et al. 2003). Consistently, β-MyHC in the NTG_{PTU} mouse would experience a 'resistive' load due to the presence of cMyBP-C, less deformation of the myofilaments and greater deformation of the nucleotide binding pocket to reduce k_{-ADP} and prolong t_{on}. In contrast, the rates of nucleotide release and binding in the α-MyHC are so fast that at physiological [MgATP] it may complete the cross-bridge cycle insensitive to the manner with which loads is borne or distributed through the myofilament lattice.

Detachment rate with increasing sarcomere length

The reduction in myosin cross-bridge detachment rate with increasing sarcomere lengths suggests increasing resistive loads on the myosin cross-bridge as the sarcomere lengthened, due to increasing passive tensions that are structurally supported by, and propagated throughout, the myofilament lattice as the sarcomere is stretched. Again, α-MyHC appears here to be much less sensitive to the changes in load that occur with myofilament structure than β-MyHC. We have reported previously a reduction in myosin detachment rate with compression of the myofilament lattice spacing in insect flight muscle (Tanner et al. 2012). We would expect, although we have not measured it directly, that the myofilament lattice is compressed with sarcomere lengthening as has been reported previously for cardiac muscle (Konhilas et al. 2002). The greater sensitivity of myosin detachment rate to SL in the t/t_{PTU} may be due to a greater compressibility of myofilament distances when cMyBP-C is absent (Palmer et al. 2011).

It is also possible that the overlap of the thin filament with the C-zone of the thick filament could influence myosin detachment rate. Assuming that thick and thin filament structures provided by Luther et al. (2008) and Burgoyne et al. (2008) are relevant to our experimental conditions, all 9 cMyBP-C stripes would overlap with the thin filament at 2.2 μm. At 2.6 to 2.8 μm ~6 to 4 cMyBP-C stripes overlap with the thin filament and there is no overlap at 3.3 μm (Pfuhl and Gautel 2012). The finding that α-MyHC detachment rate is affected relatively little by SL and independent of cMyBP-C reinforces the concept that kinetics in the α-MyHC are rather insensitive to structural attributes of the sarcomere including overlap of the thin filament with cMyBP-C. The elevated sensitivity of the β-MyHC detachment rate to SL is consistent with the detachment rate being reduced with higher structural loads that would accompany lattice compression at longer sarcomere lengths. The persistence of an enhanced detachment rate for β-MyHC at 3.3 μm, where there is no overlap of the thin filament with the C-zone, suggests that interactions with the thin filament cannot be at play. Our data do not allow us to discount the possibility that kinetics of this isoform could be sensitive to cMyBP-C via its interaction with myosin heads on the thick filament as suggested by Pfuhl and Gautel (Pfuhl and Gautel 2012).

Relevance to human cardiomyopathies

Humans express predominately β-MyHC in the ventricles. In light of our current results, we would expect the human ventricle is more sensitive to the effects of aberrant cMyBP-C. In particular, some human cardiomyopathies associated with truncation mutations of cMyBP-C are accompanied by a loss of 10–30 % of cMyBP-C (Marston et al. 2009; van Dijk et al. 2009), which according to our results may lead to an abnormally high detachment rate in these ventricles. There are no reports of dysfunction in the atria, however, which express predominately α-MyHC and therefore, according to our results, are relatively insensitive to effects of low cMyBP-C incorporation.

As an illustration of this effect in the animal model, consider that mice lacking cMyBP-C or expressing a mutant non-phosphorylated cMyBP-C (AllP-) and simultaneously expressing ~70 % β-MyHC in the ventricle do not survive more than 7 weeks after birth (Sadayappan et al. 2009), while homozygous mice completely lacking cMyBP-C and expressing predominately α-MyHC, even with up to ~20–50 % β-MyHC, can live up to a year (Carrier et al. 2004; Harris et al. 2002; McConnell et al. 1999). These observations are consistent with the current findings that cMyBP-C incorporation into the cardiac sarcomere in vivo is an influential determinant of β-MyHC function, but of relatively little consequence to α-MyHC function.

Limitations

It is important to note that our choices for control mice were based solely on the intended use of thyroid hormone to control for myosin heavy chain isoform. We expect the mice lacking cMyBP-C will carry some secondary effects due to compensatory mechanisms that likely arise in response to the primary insult. We cannot know all of the secondary effects on the sarcomeric proteins, although we have tried to minimize any effects of potentially mismatched phosphorylation profiles with pretreatment by

phosphatases (Wang et al. 2013). It is expected, although not guaranteed, that the resulting secondary effects are negligible compared to those effects that are directly associated with the loss of cMyBP-C from the cardiac sarcomere. Fibrosis and myocyte disarray were present in the t/t_{T4} mouse, but not in its $WT^{t/t}_{T4}$ control. These morphological differences may have affected the magnitudes of elastic and viscous moduli in the t/t, but it would not be expected to influence the frequency characteristics of the moduli, and therefore, would not affect the measure of myosin detachment rates that were central to this study, showing similar k_{-ADP} rates for α-MyHC with and without cMyBP-C. We also report fibrosis in both the t/t_{PTU} and NTG_{PTU} control. In this pair expressing β-MyHC, the morphology was better matched yet the k_{-ADP} rates were significantly different. We would infer then that any differences in structural morphology between the mice lacking cMyBP-C and their respective controls are negligible in affecting the myosin detachment rates compared to the effects of the lack of cMyBP-C in the cardiac sarcomere.

We must also note that there may have been some irreversible damage done to the sarcomere and lattice structure at sarcomere lengths longer than 2.8 μm. The characteristic peak of myosin cross-bridge kinetics in the viscous modulus (Fig. 5e, f), however, demonstrates that cross-bridges were binding and cycling despite myofilament disarray and a loss of overlap of the thin filament with the C-zone. According to Luther et al. (2008), we would expect ~300 nm of the ~730 nm force-producing length of the thick filament to form cross-bridges at 3.3 μm. Our results at 3.3 μm, therefore, represent the effects of cross-bridge cycling without the influence of cMyBP-C's interaction with the thin filament.

Conclusion

Our findings suggest that cMyBP-C influences myosin cross-bridge kinetics in an isoform-dependent manner. Any other possible influence of cMyBP-C on sarcomere function, such as thin filament regulation or providing viscous drag, however, cannot be discerned from the current set of data. Our findings suggest that under normally high MgATP concentrations above 5 mM (Ingwall and Weiss 2004) a loss of cMyBP-C as might underlie human familial cardiomyopathy (Marston et al. 2009; van Dijk et al. 2009) could shorten cross-bridge t_{on} and enhanced mechanical performance in the slow β-MyHC typically expressed in human ventricles. Such an enhancement of cardiac contractile function might underlie the induction of hypertrophic cardiomyopathies in humans as has been suggested based on the enhanced functional effects of mutant myosins underlying hypertrophic cardiomyopathies (Debold et al. 2007; Marston et al. 2012).

Acknowledgments This work was supported by a Grant from the NIH P01 HL59408.

References

Bhuiyan MS, Gulick J, Osinska H, Gupta M, Robbins J (2012) Determination of the critical residues responsible for cardiac myosin binding protein C's interactions. J Mol Cell Cardiol 53:838–847

Burgoyne T, Muhamad F, Luther PK (2008) Visualization of cardiac muscle thin filaments and measurement of their lengths by electron tomography. Cardiovasc Res 77:707–712

Campbell K, Chandra M, Kirkpatrick R, Slinker B, Hunter W (2004) Interpreting cardiac muscle force-length dynamics using a novel functional model. Am J Physiol Heart Circ Physiol 286:H1535–H1545

Carrier L, Knöll R, Vignier N, Keller DI, Bausero P, Prudhon B, Isnard R, Ambroisine ML, Fiszman M, Ross J, Schwartz K, Chien KR (2004) Asymmetric septal hypertrophy in heterozygous cMyBP-C null mice. Cardiovasc Res 63:293–304

Debold EP, Schmitt JP, Patlak JB, Beck SE, Moore JR, Seidman JG, Seidman C, Warshaw DM (2007) Hypertrophic and dilated cardiomyopathy mutations differentially affect the molecular force generation of mouse alpha-cardiac myosin in the laser trap assay. Am J Physiol Heart Circ Physiol 293:H284–H291

Freiburg A, Gautel M (1996) A molecular map of the interactions between titin and myosin-binding protein C. Implications for sarcomeric assembly in familial hypertrophic cardiomyopathy. Eur J Biochem 235:317–323

Godt RE, Lindley BD (1982) Influence of temperature upon contractile activation and isometric force production in mechanically skinned muscle fibers of the frog. J Gen Physiol 80:279–297

Gruen M, Gautel M (1999) Mutations in beta-myosin S2 that cause familial hypertrophic cardiomyopathy (FHC) abolish the interaction with the regulatory domain of myosin-binding protein-C. J Mol Biol 286:933–949

Harris SP, Bartley CR, Hacker TA, McDonald KS, Douglas PS, Greaser ML, Powers PA, Moss RL (2002) Hypertrophic cardiomyopathy in cardiac myosin binding protein-C knockout mice. Circ Res 90:594–601

Hofmann PA, Greaser ML, Moss RL (1991) C-protein limits shortening velocity of rabbit skeletal muscle fibres at low levels of Ca2+ activation. J Physiol 439:701–715

Hunter PJ, McCulloch AD, ter Keurs HE (1998) Modelling the mechanical properties of cardiac muscle. Prog Biophys Mol Biol 69:289–331

Ingwall JS, Weiss RG (2004) Is the failing heart energy starved? On using chemical energy to support cardiac function. Circ Res 95:135–145

Kad NM, Patlak JB, Fagnant P, Trybus KM, Warshaw DM (2007) Mutation of a conserved glycine in the SH1–SH2 helix affects the load-dependent kinetics of myosin. Biophys J 92:1623–1631

Kawai M, Halvorson H (1991) Two step mechanism of phosphate release and the mechanisms of force generation in chemically skinned fibers of rabbit psoas muscle. Biophys J 59:329–342

Konhilas JP, Irving TC, de Tombe PP (2002) Myofilament calcium sensitivity in skinned rat cardiac trabeculae: role of interfilament spacing. Circ Res 90:59–65

Korte FS, McDonald KS, Harris SP, Moss RL (2003) Loaded shortening, power output, and rate of force redevelopment are

increased with knockout of cardiac myosin binding protein-C. Circ Res 93:752–758

Korte FS, Herron TJ, Rovetto MJ, McDonald KS (2005) Power output is linearly related to MyHC content in rat skinned myocytes and isolated working hearts. Am J Physiol Heart Circ Physiol 289:H801–H812

Krenz M, Sanbe A, Bouyer-Dalloz F, Gulick J, Klevitsky R, Hewett TE, Osinska HE, Lorenz JN, Brosseau C, Federico A, Alpert NR, Warshaw DM, Perryman MB, Helmke SM, Robbins J (2003) Analysis of myosin heavy chain functionality in the heart. J Biol Chem 278:17466–17474

Land S, Niederer SA, Aronsen JM, Espe EKS, Zhang L, Louch WE, Sjaastad I, Sejersted OM, Smith NP (2012) An analysis of deformation-dependent electromechanical coupling in the mouse heart. J Physiol 590:4553–4569

Luther PK, Bennett PM, Knupp C, Craig R, Padrón R, Harris SP, Patel J, Moss RL (2008) Understanding the organisation and role of myosin binding protein c in normal striated muscle by comparison with mybp-c knockout cardiac muscle. J Mol Biol 384:60–72

Luther PK, Winkler H, Taylor K, Zoghbi ME, Craig R, Padrón R, Squire JM, Liu J (2011) Direct visualization of myosin-binding protein c bridging myosin and actin filaments in intact muscle. Proc Natl Acad Sci USA 108:11423–11428

Marston S, Copeland O, Jacques A, Livesey K, Tsang V, McKenna WJ, Jalilzadeh S, Carballo S, Redwood C, Watkins H (2009) Evidence from human myectomy samples that MYBPC3 mutations cause hypertrophic cardiomyopathy through haploinsufficiency. Circ Res 105:219–222

Marston S, Copeland O, Gehmlich K, Schlossarek S, Carrier L (2012) How do MYBPC3 mutations cause hypertrophic cardiomyopathy? J Muscle Res Cell Motil 33:75–80

McConnell BK, Jones KA, Fatkin D, Arroyo LH, Lee RT, Aristizabal O, Turnbull DH, Georgakopoulos D, Kass D, Bond M, Niimura H, Schoen FJ, Conner D, Fischman DA, Seidman CE, Seidman JG, Fischman DH (1999) Dilated cardiomyopathy in homozygous myosin-binding protein-C mutant mice. J Clin Invest 104:1235–1244

Nyland LR, Palmer BM, Chen Z, Maughan DW, Seidman CE, Seidman JG, Kreplak L, Vigoreaux JO (2009) Cardiac myosin binding protein-C is essential for thick-filament stability and flexural rigidity. Biophys J 96:3273–3280

Oshima K, Sugimoto Y, Irving TC, Wakabayashi K (2012) Head-head interactions of resting myosin crossbridges in intact frog skeletal muscles, revealed by synchrotron X-ray fiber diffraction. PLoS ONE 7:e52421

Palmer BM, Noguchi T, Wang Y, Heim JR, Alpert NR, Burgon PG, Seidman JG, Seidman CE, Maughan DW, LeWinter MM (2004) Effect of cardiac myosin binding protein-C on mechanoenergetics in mouse myocardium. Circ Res 94:1615–1622

Palmer BM, Sadayappan S, Wang Y, Weith AE, Previs MJ, Bekyarova T, Irving TC, Robbins J, Maughan DW (2011) Roles for cardiac MyBP-C in maintaining myofilament lattice rigidity and prolonging myosin cross-bridge lifetime. Biophys J 101:1661–1669

Palmiter KA, Tyska MJ, Dupuis DE, Alpert NR, Warshaw DM (1999) Kinetic differences at the single molecule level account for the functional diversity of rabbit cardiac myosin isoforms. J Physiol 519:669–678

Pereira JS, Pavlov D, Nili M, Greaser M, Homsher E, Moss RL (2001) Kinetic differences in cardiac myosins with identical loop 1 sequences. J Biol Chem 276:4409–4415

Pfuhl M, Gautel M (2012) Structure, interactions and function of the N-terminus of cardiac myosin binding protein C (MyBP-C): who does what, with what, and to whom? J Muscle Res Cell Motil 33:83–94

Previs MJ, Previs SB, Gulick J, Robbins J, Warshaw DM (2012) Molecular mechanics of cardiac myosin-binding protein C in native thick filaments. Science 337:1215–1218

Razumova MV, Shaffer JF, Tu AY, Flint GV, Regnier M, Harris SP (2006) Effects of the N-terminal domains of myosin binding protein-C in an in vitro motility assay: evidence for long-lived cross-bridges. J Biol Chem 281:35846–35854

Reiser PJ, Kline WO (1998) Electrophoretic separation and quantitation of cardiac myosin heavy chain isoforms in eight mammalian species. Am J Physiol 274:H1048–H1053

Rundell VLM, Manaves V, Martin AF, de Tombe PP (2005) Impact of beta-myosin heavy chain isoform expression on cross-bridge cycling kinetics. Am J Physiol Heart Circ Physiol 288:H896–H903

Saber W, Begin KJ, Warshaw DM, VanBuren P (2008) Cardiac myosin binding protein-C modulates binding and kinetics in the in vitro motility assay. J Mol Cell Cardiol 44:1053–1061

Sadayappan S, Gulick J, Osinska H, Martin LA, Hahn HS, Dorn GW, Klevitsky R, Seidman CE, Seidman JG, Robbins J (2005) Cardiac myosin-binding protein-c phosphorylation and cardiac function. Circ Res 97:1156–1163

Sadayappan S, Gulick J, Klevitsky R, Lorenz JN, Sargent M, Molkentin JD, Robbins J (2009) Cardiac myosin binding protein-c phosphorylation in a beta-myosin heavy chain background. Circulation 119:1253–1262

Stelzer JE, Fitzsimons DP, Moss RL (2006) Ablation of myosin-binding protein-C accelerates force development in mouse myocardium. Biophys J 90:4119–4127

Tanner BCW, Daniel TL, Regnier M (2007) Sarcomere lattice geometry influences cooperative myosin binding in muscle. PLoS Comput Biol 3:e115

Tanner BCW, Farman GP, Irving TC, Maughan DW, Palmer BM, Miller MS (2012) Thick-to-thin filament surface distance modulates cross-bridge kinetics in Drosophila flight muscle. Biophys J 103:1275–1284

Tyska MJ, Warshaw DM (2002) The myosin power stroke. Cell Motil Cytoskeleton 51:1–15

van Dijk SJ, Dooijes D, dos Remedios C, Michels M, Lamers JMJ, Winegrad S, Schlossarek S, Carrier L, ten Cate FJ, Stienen GJM, van der Velden J (2009) Cardiac myosin-binding protein c mutations and hypertrophic cardiomyopathy: haploinsufficiency, deranged phosphorylation, and cardiomyocyte dysfunction. Circulation 119:1473–1483

Veigel C, Molloy JE, Schmitz S, Kendrick-Jones J (2003) Load-dependent kinetics of force production by smooth muscle myosin measured with optical tweezers. Nat Cell Biol 5:980–986

Wang Y, Tanner BCW, Lombardo AT, Tremble SM, Maughan DW, Vanburen P, Lewinter MM, Robbins J, Palmer BM (2013) Cardiac myosin isoforms exhibit differential rates of MgADP release and MgATP binding detected by myocardial viscoelasticity. J Mol Cell Cardiol 54:1–8

Weith A, Sadayappan S, Gulick J, Previs MJ, Vanburen P, Robbins J, Warshaw DM (2012) Unique single molecule binding of cardiac myosin binding protein-C to actin and phosphorylation-dependent inhibition of actomyosin motility requires 17 amino acids of the motif domain. J Mol Cell Cardiol 52:219–227

Zhao Y, Kawai M (1993) The effect of the lattice spacing change on cross-bridge kinetics in chemically skinned rabbit psoas muscle fibers. II. Elementary steps affected by the spacing change. Biophys J 64:197–210

Zoghbi ME, Woodhead JL, Moss RL, Craig R (2008) Three-dimensional structure of vertebrate cardiac muscle myosin filaments. Proc Natl Acad Sci USA 105:2386–2390